



TECHNICAL UNIVERSITY OF CLUJ-NAPOCA

ACTA TECHNICA NAPOCENSIS

Series: Applied Mathematics, Mechanics, and Engineering
Vol. 65, Issue IV, November, 2022

STUDY REGARDING THE KINEMATIC AND FUNCTIONAL ASPECTS OF GLOBOIDAL WORM GEAR

Roland NINACS, Felicia Aurora CRISTEA, Simion HARAGĂȘ

Abstract: The unconventional worm gears are an alternative variant to conventional worm gears. Their main advantages are the high efficiency and the possibility of precise positioning (by canceling the axial clearance). Nonconventional worm gears with bearings have a shape and geometry similar to the globoidal worm gear. The kinematic analysis of the globoidal gear carried out in this paper will be used later for the kinematic analysis of the nonconventional worm gear with bearings.
Key words: *unconventional worm gear, globoidal gear, gear kinematics.*

1. INTRODUCTION

The aim of the paper is to determine the kinematic parameters of a globoid worm gear.

The worm gear is a common and important mechanism in industry. It has high transmission ratio and achieving a multiplication of torque. Disadvantages include significant friction (resulting directly in low efficiency) and backlash in the gear [2], [3].

A relatively recently appeared variant is that of the nonconventional worm gear with bearings (Fig.1) in which the previously mentioned disadvantages are minimized [4], [5], [10],[11] [12], [13].



Fig. 1 Unconventional worm gear with bearings.

This gear has geometry and kinematics very similar to that of a globoidal worm gear. Starting from the kinematic analysis of the globoidal gear, one can later proceed to the kinematic study of the nonconventional worm gear with bearings.

1.1 Description of the globoidal worm gear

The brief description of the globoidal worm gear would be: the worm and the worm wheel.

The worm of the globoidal worm gear, unlike that of cylindrical worm gears, is not cylindrical in shape. The reference line in the axial plane is an arc of a circle which, in the case of perpendicular axes, overlaps the reference circle of the wheel, and its reference surface is formed by the rotation of the circle around its own axis [4]. This surface is a portion of the inner surface of a circular torus called the globoidal surface.

The ends of the spirals of the globoidal worm are also located on a globoidal surface coaxial with the reference one. Thus, not only does the worm wheel wrap around the worm, similar to cylindrical worm gears, but the worm in turn wraps around the wheel.

The shape of the globoid worm gear teeth is determined by the shape of the globoid worm turn. In the case of perpendicular axes, the worm profile in its axial section is perpendicular to the wheel axis and overlaps the wheel profile, a property that determines that the number of teeth in contact during gearing is constant and greater than in cylindrical worm gears, this representing a main advantage of the globoid gear [5], [6],[7].

2. THE GEOMETRY AND KINEMATICS OF THE GLOBOIDAL WORM GEAR WITH A RECTILINEAR PROFILE IN THE AXIAL SECTION

It considers a rectilinear profile (Fig. 3), in axial section, of the flank of the globoidal worm [6], a profile that is generated by a straight line, line *d*, contained in the plane of the circle or the reference plane, it was considered fixed. At the rotation of the line *d* around the center of this circle, with the angular velocity ω_2 and at the simultaneous rotation of the worm around its axis with the angular velocity ω_1 , the transmission ratio *i* is as follows:

$$i = i_{12} = \frac{1}{i_{21}} = \frac{\omega_1}{\omega_2} = \frac{\varphi_1}{\varphi_2} = const \quad (1)$$

It considers the moving axis systems like in the figure 2, which are the coordinates $x_1y_1z_1$ for the worm and $x_2y_2z_2$ for the wheel, as well as the fixed systems xyz for the worm and the wheel $x^*y^*z^*$ with the help of which the parametric equations can be deduced to movement:

$$\begin{aligned} x_1 &= x^* \cos \varphi_1 + (z^* + A) \sin \varphi_1 \\ y_1 &= y^* \\ z_1 &= (z^* + A) \cos \varphi_1 - x^* \sin \varphi_1 \\ x^* &= x_2 \\ y^* &= y_2 \cos \varphi_2 - z_2 \sin \varphi_2 \\ z^* &= z_2 \cos \varphi_2 + y_2 \sin \varphi_2 \end{aligned} \quad (2)$$

The kinematic parameters are highlighted in figure 2 [6]. The relative speed \bar{v} of a point M, which belongs to the wheel, compared to the same point belonging to the worm at the time of

movement [8], [9], influenced by the angle of rotation of the worm, φ_1 , and it will be:

$$\begin{aligned} \bar{v} &= \bar{v}_{21} = \bar{v}_2 - \bar{v}_1 = \\ &= \bar{\omega}_2 \times (\bar{r}_1 - \bar{A}) - \bar{\omega}_1 \times \bar{r}_1 \end{aligned} \quad (3)$$

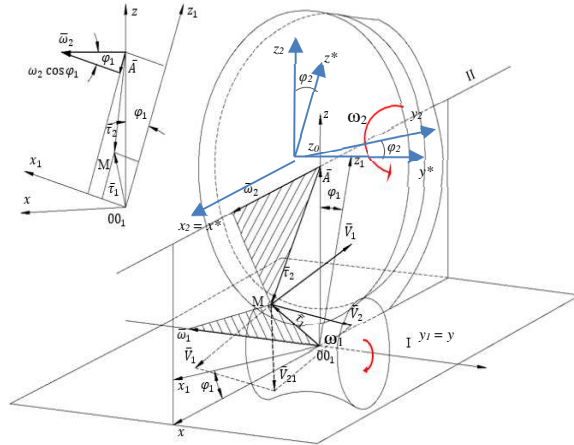


Fig. 2 Globoidal worm gear.

Projecting the equation of the mobile axes $x_1y_1z_1$ we will have:

$$\begin{aligned} \bar{v} &= \begin{vmatrix} \bar{i} & \bar{j} & \bar{k} \\ \omega_2 \cos \varphi_1 & 0 & -\omega_2 \sin \varphi_1 \\ x_1 - A \sin \varphi_1 & y_1 & z_1 - A \cos \varphi_1 \end{vmatrix} - \\ &- \begin{vmatrix} \bar{i} & \bar{j} & \bar{k} \\ 0 & -\omega_1 & 0 \\ x_1 & y_1 & z_1 \end{vmatrix} \end{aligned} \quad (4)$$

From the relation (4) results the scalar components of velocity on the mobile axes system:

$$\begin{aligned} v_{x1} &= \omega_1(z_1 + y_1 i_{12} \sin \varphi_1) \\ v_{y1} &= \omega_1 i_{21} (A - x_1 \sin \varphi_1 - z_1 \cos \varphi_1) \\ v_{z1} &= \omega_1 (i_{21} y_1 \cos \varphi_1 - x_1) \end{aligned} \quad (5)$$

Realising the correlation between relations (3) and (5), it will observe an addition:

$$n_{x1} v_{x1} + n_{y1} v_{y1} + n_{z1} v_{z1} = y_1 (n_{x1} \sin \varphi_1 + n_{z1} \cos \varphi_1) - i_{12} (n_{z1} x_2 - n_{x1} z_1) + n_{y1} (A - x_2 \sin \varphi_1 - z_1 \cos \varphi_1) = 0 \quad (6)$$

From relations (5) and (6) will result the following:

$$\begin{aligned} n_{x_1} \sin \varphi_1 + n_{z_1} \cos \varphi_1 &= u i_{21} \sin(\varphi_1 - \varphi) + \Delta \cos(\varphi_1 - \varphi) \sin(i_{21} \varphi_1 + \alpha) \\ i_{12}(n_{z_1} x_1 - n_{x_1} z_1) &= u[A - r_0 \sin(i_{21} + \alpha) - u \cos(i_{21} + \alpha)] = u \Delta \quad (7) \\ n_{y_1}(A - x_1 \sin \varphi_1 - z_1 \cos \varphi_1) &= \\ &= \Delta \cos(i_{21} \varphi_1 + \alpha) \quad [A - \Delta \cos(\varphi_1 - \varphi)] \end{aligned}$$

where:

$$\Delta = A - r_0 \sin(i_{21} \varphi_1 + \alpha) - u \cos(i_{21} + \alpha) \quad (8)$$

and

$$\varphi_1 - \varphi = \psi \quad (9)$$

In this way, replacing in the relation (6) these values and y_1 resulting of the relation (2) we will have the following:

$$\begin{aligned} u^2[(1 - \cos \psi) \cos(i_{21} \varphi_1 + \alpha) + \\ + i_{21} \sin \psi \sin(i_{21} \varphi_1 + \alpha)] + u\{r_0[(1 \\ - \cos \psi) \sin(i_{21} \varphi_1 + \alpha) - \\ - i_{21} \sin \psi \cos(i_{21} \varphi_1 + \alpha)] - A(1 - \cos \psi)[1 \\ + \cos^2(i_{21} \varphi_1 + \alpha)]\} + \\ + A \cos(i_{21} \varphi_1 + \alpha) (1 - \cos \psi)[A - r_0 \sin(i_{21} \varphi_1 + \alpha)] \\ = 0 \end{aligned} \quad (10)$$

This equation represents the addition between φ and u parameters regarding the characteristic points of the gear. All this for the angle φ_1 :

$$2 \sin \frac{\psi}{2} (Mu^2 + Nu + P) = 0 \quad (11)$$

$$M = \sin \frac{\psi}{2} \cos(i_{21} \varphi_1 + \alpha) +$$

$$i_{21} \cos \frac{\psi}{2} \sin(i_{21} \varphi_1 + \alpha)$$

$$\begin{aligned} N = r_0 \left[\sin(i_{21} \varphi_1 + \alpha) - \right. \\ \left. i_{21} \cos \frac{\psi}{2} \cos(i_{21} \varphi_1 + \alpha) \right] - A \sin \frac{\psi}{2} [1 + \\ \cos^2(i_{21} \varphi_1 + \alpha)] \end{aligned} \quad (12)$$

$$\begin{aligned} P = A \sin \frac{\psi}{2} \cos(i_{21} \varphi_1 + \alpha) [A - \\ r_0 \sin(i_{21} \varphi_1 + \alpha)] \end{aligned}$$

Based on the fact that, the mutual winding surfaces and the meshing surface can be considered generated by the characteristic curve when there is a dependency relationship between the parameters φ_1 and u , it will also represent the equation of the characteristic curve in the $x_1 y_1 z_1$ system, corresponding to the phase φ_1 . The characteristic curve defined in this way, it can also be related to the fixed system xyz of the gear wheel, thus obtaining the equation of the gear surface or to the mobile system $x_2 y_2 z_2$ related to the wheel, thus obtaining the equation of the flank of the wheel tooth. But, to arrive at these shapes with the help of the figure 3, it was considered that: $\varphi_1 = \varphi_{11}$

$$\varphi_2 = \varphi_{22} \quad (13)$$

The passing from the mobile systems $x_1 y_1 z_1$, $x_2 y_2 z_2$ at the fixe axes xyz could be make in this way:

$$\begin{aligned} x &= x_1 \cos \varphi_{11} - z_1 \sin \varphi_{11} \\ y &= y_1 \\ z &= x_1 \sin \varphi_{11} + z_1 \cos \varphi_{11} \end{aligned} \quad (14)$$

and

$$\begin{aligned} x_2 &= x^* \\ y_2 &= z^* \sin \varphi_{22} + y^* \cos \varphi_{22} \\ x^* &= x_1 \cos \varphi_{11} - z_1 \sin \varphi_{11} \end{aligned} \quad (15)$$

$$y^* = y_1$$

$$\begin{aligned} z_2 &= z^* \cos \varphi_{22} + y^* \sin \varphi_{22} \\ z^* &= x_1 \sin \varphi_{11} + z_1 \cos \varphi_{11} - A \end{aligned}$$

It taking into account: $\varphi_{22} = i_{21} \varphi_{11}$ of relation (14), we will have it:

$$\begin{aligned} x_2 &= x_1 \cos \varphi_{11} - z_1 \sin \varphi_{11} \\ y_2 &= x_1 \sin \varphi_{11} \sin i_{21} \varphi_{11} + \\ &z_1 \cos \varphi_{11} \sin i_{21} \varphi_{11} + y_1 \cos i_{21} \varphi_{11} - \\ &A \sin i_{21} \varphi_{11} \\ z_2 &= x_1 \sin \varphi_{11} \cos i_{21} \varphi_{11} + \\ &z_1 \cos \varphi_{11} \cos i_{21} \varphi_{11} - y_1 \sin i_{21} \varphi_{11} - \\ &A \cos i_{21} \varphi_{11} \end{aligned} \quad (16)$$

Replacing the values of x_1, y_1, z_1 results the surface or meshing equation of the shape gear:

$$\begin{aligned} x &= \sin \psi [A - r_0 \sin(i_{21}\varphi_1 + \alpha) - \\ &u \cos(i_{21}\varphi_1 + \alpha)] \\ y &= u \sin(i_{21}\varphi_1 + \alpha) - r_0 \cos(i_{21}\mu\varphi_1 + \alpha) \\ &\quad (17) \\ z &= \cos \psi [A - r_0 \sin(i_{21}\varphi_1 + \alpha) - \\ &u \cos(i_{21}\varphi_1 + \alpha)] \end{aligned}$$

Replacing these values x_1, y_1, z_1 in relation (15) it obtains the flank equation of the wheel tooth:

$$\begin{aligned} x_2 &= \sin \psi [A - r_0 \sin(i_{21}\varphi_{11} + \alpha) - \\ &u \cos(i_{21}\varphi_{11} + \alpha)] \\ y_2 &= u[\cos i_{21}\varphi_{11} \sin(i_{21}\varphi_1 + \alpha) - \\ &\cos(i_{21}\varphi_1 + \alpha) \cos \psi \sin i_{21}\varphi_{11}] - \\ &r_0[\cos \psi \sin i_{21}\varphi_1 \sin(i_{21}\varphi_1 + \alpha) + \\ &\cos i_{21}\varphi_{11} \cos(i_{21}\varphi_1 + \alpha)] + \\ &A(\cos \psi \sin i_{21}\varphi_{11} - \sin i_{21}\varphi_{11}) \quad (18) \\ z_2 &= -u[\cos(i_{21}\varphi_1 + \alpha) \cos i_{21}\varphi_{11} \cos \psi + \\ &\sin i_{21}\varphi_{11} \sin(i_{21}\varphi_1 + \alpha)] - \\ &r_0[\cos i_{21}\varphi_{11} \sin(i_{21}\varphi_1 + \alpha) \cos \psi - \\ &\sin i_{21}\varphi_{11} \cos(i_{21}\varphi_1 + \alpha)] - A(\cos i_{21}\varphi_{11} - \\ &\cos \psi \cos i_{21}\varphi_{11}) \end{aligned}$$

The two independent parameters that determine the gear surfaces and wheel flanks resulting from relations (17) and (18) are φ_1 and φ_{11} since the parameter ψ results as a function of μ_1 and φ_1 from relation (15). The u parameter is also obtained as a function of μ_1 and φ_1 from the quadratic equation.

$$Mu^2 + Nu + P = 0 \quad (19)$$

The equation (18) has two roots, so two meshing surfaces and two wrapped flanks will result, only one of which is compatible with the problem at hand. The given system is checked for the condition:

$$\psi = \varphi_1 - \varphi_{11} = 0 \quad (20)$$

Replacing the relation (20) into (18) will have it:

$$\begin{aligned} x &= 0 \\ y &= u \sin(i_{21}\varphi_1 + \alpha) - r_0 \cos(i_{21}\varphi_1 + \alpha) \quad (21) \\ z &= A - r_0 \sin(i_{21}\varphi_1 + \alpha) - u \cos(i_{21}\varphi_1 + \alpha) \end{aligned}$$

or

$$\begin{aligned} x &= 0 \\ z &= -y \cot(i_{21}\varphi_1 + \alpha) + A - \frac{r_0}{\sin(i_{21}\varphi_1 + \alpha)} \quad (22) \end{aligned}$$

Relation (22) presents us the lines family that are tangent of the profile circle, the lines contained in the plane $x = 0$.

It will replace $\psi = 0$ into relation (18):

$$\begin{aligned} x_2 &= 0 \\ y_2 &= u \sin \alpha - r_0 \cos \alpha \quad (23) \\ z_2 &= -u \cos \alpha - r_0 \sin \alpha \end{aligned}$$

or

$$\begin{aligned} x_2 &= 0 \\ z_2 &= -y_2 \cot \alpha - \frac{r_0}{\sin \alpha} \quad (24) \end{aligned}$$

Relation (24) represents the equation of the generating line in the plane $x_2 = 0$.

Thus, in globoid gears with rectilinear profiles in the axial section, there are two surfaces of engagement, one of which merges with the plane of the generating line in the median plane of the wheel, and the other is the surface given by the equation of the surface of engagement, relation (24). But also the flank wrapped has two parts, an edge that merges with the generating line and a surface given by equations (24).

It is important to note that, these aspects can also be reached in an intuitive way. So, first determine the variation of the helix angle given by the intersection of the flank of the globoidal beaver of the torus, with the radius of the generating circle

$$R = \sqrt{r_0^2 + u^2}.$$

Taking into account the variation of the radius of curvature of the flank section with a plane P,

perpendicular to the generating line at the point M, at the distance R from the center of the wheel, which distance is equal to the radius of the generating circle of the torus (Fig.3).

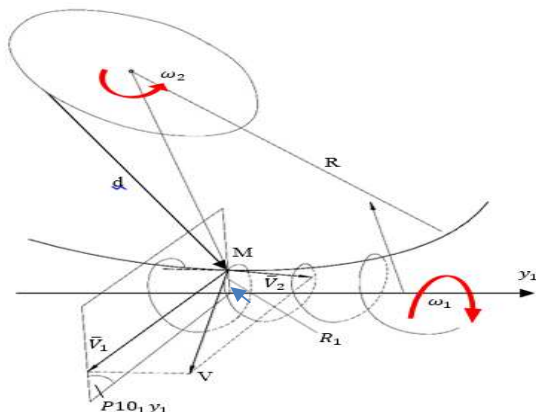


Fig. 3 Kinematic parameters.

In the figure 3, the helix is described by the point M of the generating line which moves on the helix with the speed \bar{v} and which coincides with the direction of its tangent having two components:

$$v_2 = R\omega_2 \quad (25)$$

$$v_1 = R_1\omega_1$$

Where R_1 is the variable distance of M relative to the 0_1y_1 axis.

Taking into account what was explained previously, the following relationship results:

$$\tan \theta = \frac{v_2}{v_1} = \frac{R\omega_2}{R_1\omega_1} = \frac{R}{R_1} i_{21} \quad (26)$$

In this way, it will result that the helix pitch angle θ varies along the axis of the screw and has minimum values at the ends and maximum value in the throttle section.

3. CONCLUSIONS

The kinematics of the globoidal worm gear is quite complex, being an important and mandatory step in establishing a mathematical model of this type of gear, a model that also takes into account dynamic aspects. Among the classic worm gears, the globoid worm gear, it is closest in shape and geometry to non-conventional worm gears.

The kinematic analysis of the globular gear will be used later for the kinematic analysis of the nonconventional worm gear with bearings. Regardless of the type of gear, an important factor is its performance. For the performance of a gear, the bearing capacity, the vibrations in the mechanism, the noise it produces, the working temperature, the heating of the gear are analyzed it. These represent energy losses leading to a decrease in the efficiency of the mechanism. If the fields of application of worm gears are to be considered, when high precision is desired, they can be replaced by worm gears with bearings (nonconventional), which come with several advantages such as: the worm gear with bearings has eliminate the backlash between the worm wheel and the worm and replace the sliding friction between the spiral worm and the worm gear teeth with the rolling friction between the spiral worm and the bearings.

All this leads to the need for a lower actuation force, increasing in this way the efficiency and also the life of the gear.

4. REFERENCES

- [1] Bălcău, Monica, Cristea A.F., (2019). *Theoretical considerations regarding the dynamic absorber*. Acta Technica Napocensis, Series: Applied Mathematics, Mechanics, and Engineering, Vol. 61, Issue III, September, 2018, pg. 323-332, Editura U.T.PRESS, ISSN 1221-5872.
- [2] Monica Bălcău, Mariana Arghir, *The replacement of the pendular dynamic absorber with a rotating mass*, în Acta Technica Napocensis, 2011, seria Applied Mathematics and Mechanics, nr. 54, vol. I, ISSN 1221-5872, pag.91-94.
- [3] Deng, X., Wang, J., Wang, S., Liu, Y. – *Investigation on the Backlash of Roller Enveloping Hourglass Worm Gear: Theoretical Analysis and Experiment*, Mississippi State University, 2018.
- [4] Haragâș, S. – *Organe de mașini*, Editura Napoca Star, 2014, Cluj-Napoca.
- [5] Haragâș, S. – *Reductoare cu o treaptă. Calcul și proiectare*, Editura Risoprint, 2014, Cluj-Napoca.

- [6] Maros, D. – Angrenaje melcate, Editura Tehnică, 1966, București
- [7] Ninacs, R. - *Angrenaje melcate neconvenționale*, raport de cercetare, IOSUD-UTCN 2022.
- [8] Schonstein, C. – *Considerations about matrix exponentials in geometrical modeling of the robots*, Acta Technica Napocensis, Series: Applied Mathematics, Mechanics, and Engineering, Issue 2, No. 62, June, 2019, Cluj-Napoca, ISSN 1221-5872.
- [9] Schonstein, C. – *Kinematic control functions for a serial robot structure based on the time derivative Jacobian matrix*, Acta Technica Napocensis, Series: Applied Mathematics and Mechanics, No. 61, Issue II, 2018, Cluj-Napoca, ISSN 1221-5872, Romania.
- [10] Sedgwick, R. – *Recirculating ball worm drive*, Wisconsin, 1968.
- [11] Vyatkin, A. – *Analysis of the geometry and contact density of globoid gearing*, MATEC Web of Conferences 329, 03008 (2020) <https://doi.org/10.1051/mateconf/202032903008>, ICMTMTE 2020.
- [12] <https://www.nikken-kosakusho.co.jp/en/product/index.php?seq=42>
- [13] <https://www.semanticscholar.org/paper/Innovative-Design-for-A-Ball-Worm-Gear-Mechanism-Kocak/687de07f9e3ad543171689a4686e94d5f514bc94/figure/7>

Studiu privind aspectele cinematice și funcționale la angrenajul melcat globoidal

Rezumat: Angrenajele melcate neconvenționale sunt o variantă viabilă de înlocuire a angrenajelor melcate clasice. Principalele avantaje ale acestora sunt randamentul ridicat și posibilitatea poziționărilor precise (prin anulare jocului axial). Angrenajele melcate neconvenționale cu rulmenți au o formă și o geometrie asemănătoare angrenajului melcat globoidal. Analiza cinematică a angrenajului globoidal realizată în cadrul acestei lucrări, va fi utilizată ulterior pentru analiza cinematică a angrenajului melcat neconvențional cu rulmenți.

Roland NINACS, Ph.D. student, Technical University of Cluj-Napoca, Faculty of Industrial Engineering, Robotics and Production Management, Romania, e-mail: ninacs_roland@yahoo.com

CRISTEA A. Felicia, Ass. Professor Ph.D. Eng., Technical University of Cluj-Napoca, Faculty of Industrial Engineering, Robotics and Production Management, Mechanical Engineering Department, Romania, e-mail: felicia.cristea@mep.utcluj.ro

Simion HARAGĂȘ, Professor Ph.D. Eng. Technical University of Cluj-Napoca, Faculty of Industrial Engineering, Robotics and Production Management, Mechanical Engineering Department, Romania, e-mail: Simion.Haragas@omt.utcluj.ro